Melbourne Graduate Fluids Conference, 2001
Monash University, Melbourne, Australia

A 2D NUMERICAL STUDY OF THE FLOW AROUND BLUFF RINGS

G.J. SHEARD, M.C. THOMPSON and K. HOURIGAN

Department of Mechanical Engineering
Monash University, Clayton, Victoria, AUSTRALIA

ABSTRACT

A numerical study of the flow around bluff rings at low Reynolds number is presented. A Spectral Element method is used to solve the unsteady axisymmetric Navier-Stokes equations governing the fluid flow. Strouhal-Reynolds number profiles are provided for a range of ring aspect ratios, as well as critical Reynolds numbers for the onset of flow separation and periodic flow. These results show a decrease in shedding frequency and an increase in the critical Reynolds numbers for separation and unsteady flow with decreasing ring aspect ratio.

1. INTRODUCTION

Bluff body flows have been of practical interest to mankind for centuries. Be it the mechanics of ships or aircraft, the trajectory of an arrow or cannonball, the flow of a fluid (air, water, or another medium) around a body and the interaction that takes place, all of these are of immense interest.

Research has shown for various bluff bodies that a variety of flow states to exist over a range of Reynolds number. Very low Reynolds number flows are laminar in nature, and increasing Reynolds number leads to separation from the body and wake recirculation. The wake becomes progressively unsteady and three-dimensional with further Reynolds number increases, before becoming turbulent. Flow properties relating to drag, lift and Strouhal number vary greatly depending on the form of the wake present in the flow.

Bluff rings have been afforded little attention from researchers despite exhibiting similarities to simple geometries such as straight cylinders or spheres when the ring cross-section is extremely thin or thick respectively. Leweke & Provansal (1994) studied large aspect ratio rings due to their similarity to straight cylinders without the end effects normally encountered in experimental work. This investigation focuses on the low Reynolds number, 2D flow regime. A Galerkin Spectral-Element method is used to solve the unsteady 2D axisymmetric Navier-Stokes equations for a range of bluff ring models, with the intention of developing Strouhal profiles for the system where unsteady flow is observed, as well as determining the critical Reynolds numbers for the onset of separation of flow around the ring, and unsteadiness in the wake.

Little work has been carried out on the bluff ring geometry to date. Roshko (1953) carried out early work, noting a reduction in Strouhal number by a few percent for ring vortex shedding when compared to the straight cylinder, and pointed out some major changes experienced at low aspect ratios. Probably the most significant body of work has been contributed by Leweke & Provansal (1994). They carried out detailed experiments on bluff rings of large aspect ratio in an attempt to model cylinders without end effects. The effect of ring curvature was linearised and incorporated into an equation that provides the laminar, Strouhal-Reynolds number relationship for large-Ar bluff rings as a function of Re, curvature K and shedding angle θ:

$$St(\mathrm{Re}, K, \theta) = \{S_0(\mathrm{Re}, K = 0) - a(\mathrm{Re} - \mathrm{Re}_1)K\}\cos\theta \qquad (1)$$

$$where\ S_0(\mathrm{Re}, K = 0) = \frac{-3.810}{\mathrm{Re}} + 0.1904 + 1.220\times10^{-4}\,\mathrm{Re} \qquad (2)$$

This investigation focuses on the axisymmetric flow regime experienced at low Reynolds number. From understanding of straight cylinder and sphere flows, 3D flow appears between $178 < Re < 211$. This investigation covers the Reynolds number range up to $Re = 250$ to cover the likely 2D regime.

2. NUMERICAL METHOD

To model the bluff ring flow a Galerkin Spectral-Element scheme was used. This technique has been applied successfully to two- and three-dimensional bluff body flow problems such as the circular cylinder (Thompson et al, 1996). Briefly, the method uses a three-step time splitting scheme for temporal discretisation of the governing Navier-Stokes equations. Spatial discretisation is performed using a Galerkin Finite Element method with high-order Lagrangian interpolants applied within each element. A visual representation of the bluff ring geometry is given in **Figure 1**.

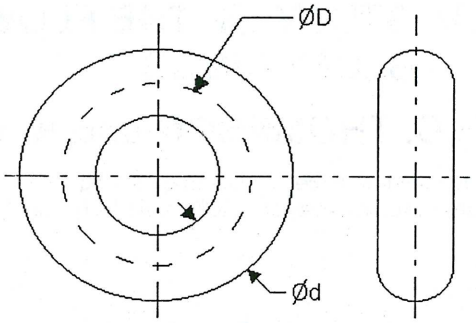

Figure 1 : Bluff ring geometry and associated dimensions.

Figure 1 shows that the geometry is essentially a torus, or a ring around the axis with a circular cross-section. The direction of fluid flow is in the axial direction, normal to the plane of the ring. The fluid flow interacts with the geometry by flowing around the circular ring cross-section, so a dimensionless parameter describing the fluid motion as a Reynolds number can be given based on the fluid velocity, U, the length scale of the ring cross-section diameter, d, and the fluid viscosity, ν:

$$Re = \frac{Ud}{\nu} \tag{3}$$

For consistency with previous studies, the geometry is represented by an aspect ratio parameter Ar. This is simply a ratio of the circumference of the ring around the axis (the major axis dimension), and the ring cross-section diameter (the minor axis dimension):

$$Ar = \frac{\pi D}{d} \tag{5}$$

3. BLUFF RING GRID RESOLUTION STUDY

A thorough grid resolution study was conducted on a family of similar grids – small Ar grids were a subset of larger Ar grids. A similar grid resolution study to that performed by Barkley & Henderson (1996) was carried out. Mesh elements were concentrated around the ring cross-section, and the downstream region, where fine resolution was required. Uniform meshes with the same concentration near the cross-section of the ring resulted in far less efficient simulations, however the discrepancy between the results of the two grids was in the order of 0.1%. Thus the grids with the tetrahedral expansion were selected for the study:

Initial studies were performed on a grid of moderate domain size and a low number of nodes per element, for the $Ar = 20\pi$ case. This was chosen because vortex shedding was expected at the chosen Re for simulation of 200, similar to the circular cylinder.

A suitable time step was found by running a simulation on the $Ar = 20\pi$ test grid with 25 nodes per element. Due to the nature of the spectral element model chosen, good temporal accuracy is achieved with the time step chosen close to the Courant time step. Convergent simulations were obtained with a time step of 0.005 for the range of Reynolds numbers being investigated in this study.

The number of nodes per element (N) chosen was found by using the $Ar = 20\pi$ grid above with the 0.005 time step, and varying the number of nodes per element. **Table 1** shows adequate performance of the $N = 49$ grid:

Nodes per element:	Strouhal number:	Percentage difference:
25	0.17813	5.8
49	0.17911	0.033
81	0.17917	0.0

Table 1 : Strouhal numbers from nodes per element study.

With a suitable time step and number of nodes per element determined, an adequate domain size was found in the radial direction to limit blockage effects caused by the outer boundary.

Previous studies on the wakes of spheres (Tomboulides et al, 1993), and cylinders (Barkley & Henderson, 1996) have found using similar numerical schemes that the transverse domain must be greater than about 12 length units from the object in 2D (ie. about 360d for the Ar = 20π ring), however variations in the radial direction for an axisymmetric model were found to vary with the square of the radius, thus requiring a smaller radial domain size based on the outer diameter of the model. **Figure 2** shows the Strouhal number found for the domain sizes tested for the $Ar = 20\pi$ case. The difference between the radius = 150d and 250d cases was a mere 0.0514%:

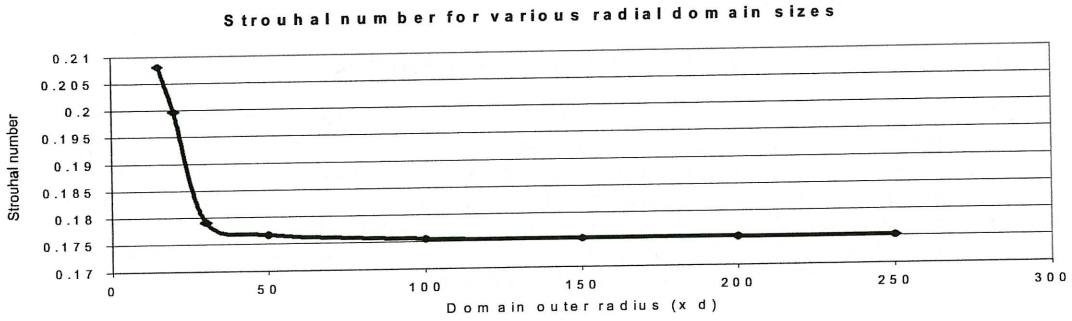

Figure 2 : Graph of Strouhal number for various radial domain sizes.

Thus the domain size of 150d units in radius was used for all aspect ratio models, and the similar mesh created for a comparative study of the straight circular cylinder.

To avoid outlet effects interfering with the wake of the ring cross-section, a downstream domain length of 25d was used, consistent with previous numerical studies such as Barkley & Henderson (1996).

4. BLUFF RING LAMINAR FLOW REGIME

The Strouhal profile for each ring in the laminar flow regime is shown in **Figure 3**. Note how the smaller Aspect ratio rings shed at lower frequency and the critical Reynolds number for the onset of shedding increases:

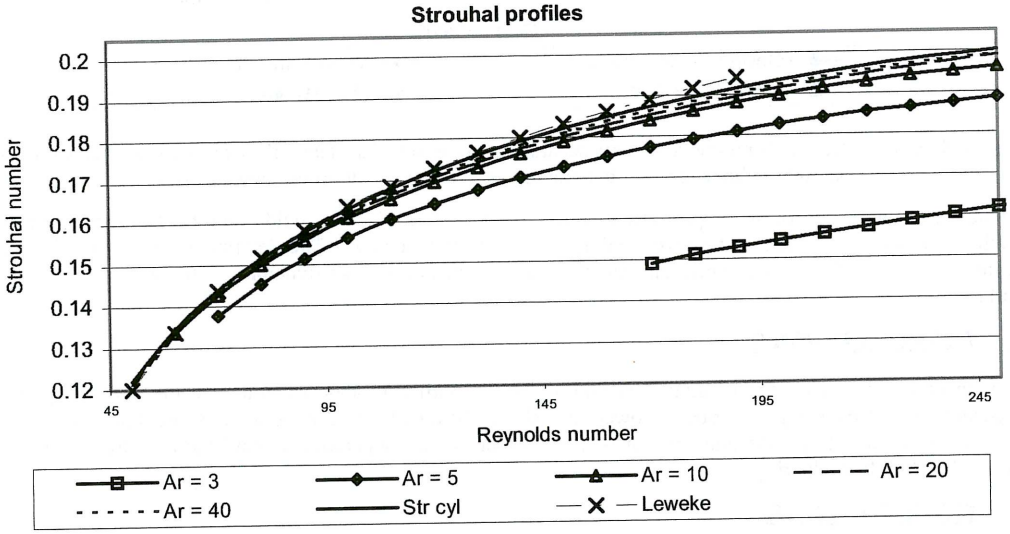

Figure 3 : Laminar Strouhal number profiles for various Aspect ratio rings, the straight circular cylinder, and results provided in the literature.

Figure 4 shows vorticity contours of the $Ar = 5\pi$ ring at $Re = 150$. Simulations such as this were conducted to ascertain the Strouhal-Reynolds profiles (see **Figure 3**) for the various ring sizes investigated. Note the pairing of shed vortices downstream of the ring, and the divergence of the vortices from the axis:

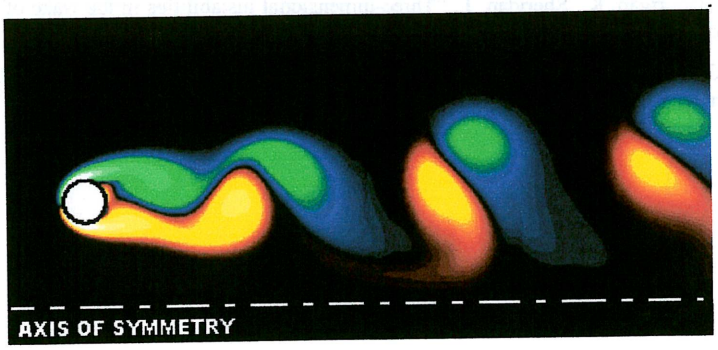

Figure 4 : Vorticity contours for flow around a bluff ring with Ar = 5π at Re = 150.

5. BLUFF RING CRITICAL REYNOLDS NUMBERS

Figure 5 illustrates a trend apparent with decreasing Aspect ratio and increasing curvature (K) for the critical Reynolds numbers for the separation of flow over the body and the onset of shedding to occur at a greater value. Curvature is related to Aspect ratio by the relation $K = 2\pi/Ar$. As expected, increasing Aspect ratio (decreasing K) represents a trend towards the limit of the geometry as a straight cylinder (left axis on chart), and the onset of shedding asymptotes towards the onset of shedding for the straight cylinder. The critical Reynolds numbers for the onset of Mode A and Mode B 3D shedding are also given for the straight cylinder case. Future work will complete the trend of such 3D instabilities over the bluff ring parameter space.

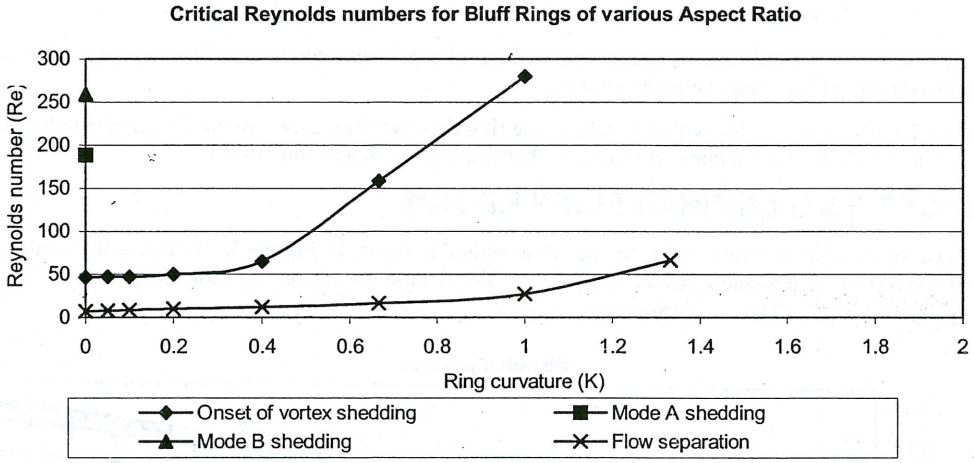

Figure 5 : Critical Reynolds numbers for flow separation and onset of unsteady flow for increasing ring curvature (straight cylinder on left, tending towards a sphere with increasing curvature.

3D flow is expected to occur in preference to the axisymmetric 2D flow fields investigated here at Reynolds numbers of order Re = 200 and above, leading to fully turbulent flow. The determination of both the critical Reynolds numbers for such a transition, and the resulting physical wake dynamics is the topic of forthcoming work.

6. CONCLUSIONS

As with previous studies, the laminar flow regime for the bluff ring appears similar to the straight cylinder at sufficient Ar. Decreasing Ar tends to lower the relative Strouhal number for a given Reynolds number, and increase the critical Reynolds numbers for both the onset of flow separation around the ring cross-section, and vortex shedding from the ring.

7. REFERENCES

Barkley, D., Henderson, R. D., "Three-dimensional Floquet stability analysis of the wave of a circular cylinder", *J. Fluid Mech.*, **322**, 215-241, 1996.

Leweke, T., Provansal, M., "The flow behind rings: bluff body wakes without end effects", *J. Fluid Mech.*, **288**, 265-310, 1995.

Roshko, A., "On the development of turbulent wakes from vortex streets", *NACA Tech. Note 2913*, 1953.

Thompson, M.C., Hourigan, K., Sheridan, J., "Three-dimensional instabilities in the wake of a circular cylinder", *Exp. Therm. Fluid Sci.*, **12**, 190-196, 1996.

Tomboulides, A.G., Orszag, S.A., Karniadakis, G.E., "Direct and large-eddy simulation of the flow past a sphere", *2nd ICTME*, Florence, 1993.